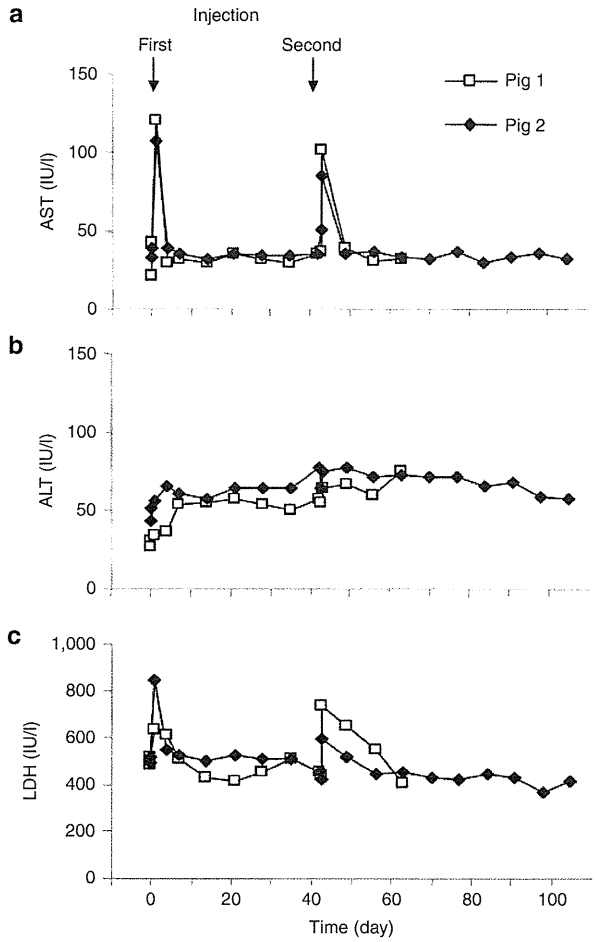

Figure 5 Effect of hydrodynamic gene delivery on serum concentrations of marker enzymes. Blood samples were collected from the ear vein or peripheral vein in the limb of animals before (time = 0), 2 hours, 1, 4, 7, 14, 21, 28, 35, 42 (the day when the second injection was administered), 43, 49, 56, and 63 days after the first injection from pig 1 and 2 and as well as 70, 77, 84, 91, 98, and 105 days after the first injection from pig 2. Concentrations of (**a**) aspartate aminotransferase (AST), (**b**) alanine aminotransferase (ALT), (**c**) and lactate dehydrogenase (LDH). Arrows indicate first and second injection on day 0 and 42. The white square and black diamond-shape represent results of pig 1 and pig 2, respectively.

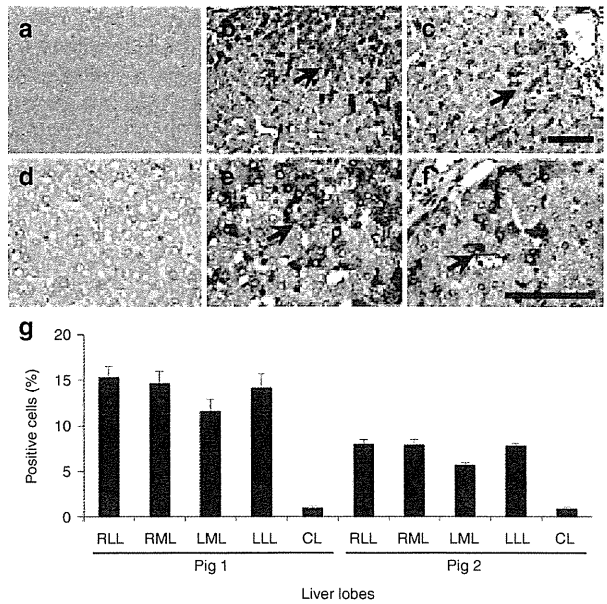

Figure 6 Persistent expression of human α-1 antitrypsin in the hepatocytes. Immunohistochemical staining of human α-1 antitrypsin was performed in the liver after the hydrodynamic gene delivery of pCAG-hAAT plasmid. (**a, d**) Noninjected CL in pig 1; (**b, e**) injected RML in pig 1; (**c, f**) injected RML in pig 2. Scale bar represents 100 μm (**a, b, c**, 200×; **d, e**, f, 400×). Black arrows represent positively stained hepatocytes. (**g**) Quantitative analysis of positively stained cells. Ten liver tissue samples collected from each lobe (total of 50 samples in a liver) in pigs 1 and 2 and a quantitative analysis was performed on three fields (total of 150 fields in a liver) from each section. The values represent mean ± SD ($n = 30$ for each lobe). $P < 0.05$ between all injected lobes and CL. One-way ANOVA followed by Bonferroni's multiple comparison test.

stained cells in the injected RLL (**Figure 6b,e**), RML, LLL, and noninjected LML, respectively, and less than 1% positive cells were found in the noninjected CL (**Figure 6a,d**) 3 weeks after injection (**Figure 6g**). The number of hAAT-expressing hepatocytes slowly decreased to 8.0, 7.9, 5.6, and 7.8% in the RLL (**Figure 6c, f**), RML, LML, and LLL, respectively, during the following 9 weeks after the second gene delivery (**Figure 6g**). These results suggest that hAAT expression in injected hepatocytes lasted 2 months after hydrodynamic gene delivery, and that the procedure could be carried out repeatedly with reasonable gene delivery efficiency.

Plasmid distribution

PCR analysis of DNA isolated from multiple organs from pigs 1 and 2 were conducted to determine whether the hAAT plasmid was delivered to organs other than the liver. A pair of ampicillin-resistant (*Amp*) gene-specific primers was utilized to detect the hAAT-expressing plasmid DNA using the glyceraldehyde 3-phosphate dehydrogenase (*Gadph*) gene as an internal control (**Figure 7**). The PCR product of *Amp* is a 660-nucleotide fragment that was detected in the injected liver lobe in pigs 1 and 2 (**Figure 7**, lane 3), but was not present in the liver of pigs who were not injected with the plasmid (**Figure 7**, lane 2). The spleens, kidneys, brains, hearts, stomachs, colons, ovaries, lungs, muscles, and small intestines of injected pigs showed no presence of the *Amp* gene. These results demonstrate that the procedure carried out in the liver did not result in gene transfer to cells in other organs, confirming the target specificity of image-guided gene delivery to the liver.

Structural impact of the lobe-specific gene transfer

Hematoxylin & eosin staining was utilized to evaluate the impact of hydrodynamic injection on hepatocytes and the surrounding tissue at appropriate time points after the injection (**Figure 8a–f**). Significant enlargement of the central vein and sinusoid was observed immediately after the injection in the injected lobe (**Figure 8d**) with same setting as in the previous section; this enlargement started to subside after 4 hours (**Figure 8e**) and completely subsided after 24 hours (**Figure 8f**). Tissue damage was not observed in the noninjected CL (**Figure 8a,b,c**). In addition, chronic liver injury or

accumulation of lymphocytes was not observed in pigs 1 and 2 in the long-term study (data not shown). These results suggest that our image-guided hydrodynamic gene delivery is safe and that the procedure could be carried out repeatedly on the same animal.

Discussion

Various methods of gene delivery have been studied, and a few have been clinically used for the treatment of diseases such as hemophilia and cancers.[17] Among the various established methods, hydrodynamic gene delivery is relatively new and was first reported in 1999 by Liu *et al.*[3] and Zhang *et al.*[4] The biggest challenge over the last few years has been in the identification of the factors and parameters that have important roles in determining the safety and efficiency of hydrodynamic gene delivery to the liver. Previously, we and others have reported that hydrodynamic gene delivery can be applied for gene delivery to the liver, muscle, and kidney in small pigs and rabbits.[7–12,18] Of note, Herrero *et al.* have demonstrated in a more recent study that effective hydrodynamic gene delivery is also achievable *ex vivo* in the human liver.[13] A primary reason that the small size animals were used in the earlier studies is that they are easier to handle. However, the drawback in using these animals is that they appear too small for being used for the development of parameters clinically applicable. For example, in 20 kg pigs, the only catheter placement in the hepatic veins is the "proximal" site and the blood vessels at the intermediate and distal sites cannot be effectively examined, because they are too small for balloon catheter. Therefore, we employed larger pigs (40–65 kg) in the current study and assessed the effect of various parameters on gene delivery efficiency and potential tissue damage. We demonstrate that optimal gene delivery can be achieved by sequential injection of individual lobes by lodging a balloon catheter in the intermediate site of the hepatic vein at an intravascular pressure of 150 mmHg and a total volume of approximately 4% body weight shown in **Figures 2** and **3**. We also demonstrate that the same procedure repeatedly applied in the same animals with identical plasmids results in long-term gene expression in hepatocytes for at least 2 months without noticeable adverse effects (**Figure 6**).

Our results indicate that insertion and placement of the catheter under fluoroscopic image are important in the impact of injection, the efficiency of gene delivery, and the safety of the procedure. Further optimization of the injection volume achieved sequential lobe-specific hydrodynamic gene delivery targeting the entire liver with no evident plasmid in other organs (**Figure 7**). Serum levels of aspartate aminotransferase, alanine aminotransferase, and lactate dehydrogenase peaked at 24 hours and returned to normal ranges 4 days after the injection, as previously reported.[9,10] The level of the elevation was lower than that of hydrodynamic gene delivery targeting the entire liver with IVC-clumped,[12] and that of pseudo-hydrodynamic injection of helper- dependent adenoviral vectors with IVC-occlusion.[19] Therefore, our procedure of

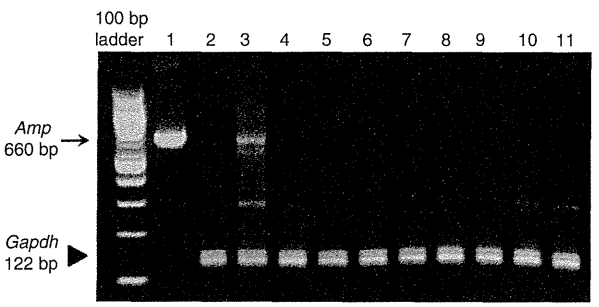

Figure 7 Tissue distribution of plasmid DNA. Multiplex PCR analysis was performed on genomic DNA collected from pigs by 35 cycles of PCR amplification using primers for ampicillin resistance (*Amp*) and glyceraldehyde 3-phosphate dehydrogenase (*Gapdh*) genes, respectively. Lanes: 1, plasmid DNA; 2, normal liver without plasmid injection; 3, injected lobe in pig 2; 4, spleen; 5, kidney; 6, brain; 7, heart; 8, stomach; 9, colon; 10, ovary; 11, lung. The arrow represents the 660 bp *Amp* fragment. The arrowhead represents the 122 bp *Gapdh* fragment.

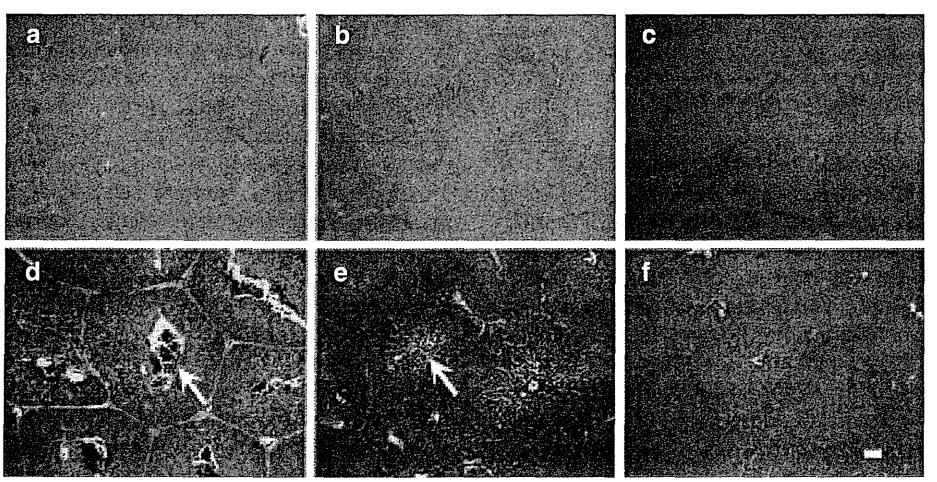

Figure 8 Assessment of tissue damage by histochemistry. Hematoxylin & eosin staining of liver samples from CL (**a**–**c**), and RML (**d**–**f**). Samples were collected immediately following the injection (**a**, **d**), 4 hours after the injection (**b**, **e**), and 24 hours after the injection (**c**, **f**). Scale bars represent 100 μm. White arrows represent central vein in the lobular structure.

catheter-based, lobe-specific hydrodynamic gene delivery is more desirable for clinical application.

Our long-term study shows approximately 10% of the hAAT-positive hepatocytes 2 months after gene transfer. The level was the same as positive hepatocytes 4 months after the injection in mice reported by Alino *et al.* using a pTG7101 plasmid containing the full length of *hAAT*.[20] If the same level of efficiency of gene delivery can be achieved in patients with α-1 antitrypsin deficiency, we expect that the amount of normal hAAT protein in hepatocytes will compete with the abnormal mutated gene product for transcription and translation. Hence, it will result in a decrease of the accumulation of abnormal hAAT protein in hepatocytes, thereby reverting liver injury in hAAT-deficiency patients.[21] Also, our successful hepatocyte-specific gene transfer suggests the promising option of transferring the gene expressing the protein that blocks the polymerization of mutant hAAT protein.[21]

It is important to note that our ELISA system was unable to detect hAAT in pig serum, whereas Alino *et al.* reported a serum level of 0.2 μg/ml of hAAT in pigs.[10] They also observed a sustained therapeutic level at 1,000 μg/ml in mice[23] using pTG7101, whereas we observed 100-fold lower levels in our study in mice.[22] Therefore, the hAAT protein level in serum in this study using our plasmid might be below detection limit of ELISA (<1 ng/ml). This is likely due to the difference of the promoter, as TG7101 contains natural promoter for *hAAT* gene whereas our plasmid was driven by chicken β-actin promoter with CMV enhancer. Alternatively, it is also possible that the hAAT expressed are not secreted effectively by swine hepatocytes. Evidently, as serum hAAT is essential for the treatment of lung disease in hAAT deficiency,[23] our work falls short in demonstrating therapeutic levels of hAAT, and additional studies are needed.

In summary, we identified factors affecting image-guided hydrodynamic gene delivery in human-size animals, and developed a clinically applicable procedure for liver-specific hydrodynamic gene delivery. Development of an automatic injector that can adjust injection pressure precisely to reproduce intravascular pressure and gene delivery efficiently may help physicians put this protocol into practice. Assessment of the applicability of this procedure in nonhuman primates that have more human-like livers is the next step toward clinical applications.

Materials and methods

Materials. The pCMV-Luc plasmid containing firefly luciferase cDNA driven by a CMV promoter and the pCAG-hAAT plasmid containing human α-1 antitrypsin gene driven by a chicken β-actin promoter with CMV enhancer, were purified by the CsCl-ethidiumbromide density gradient ultracentrifugation and kept in Tris-EDTA buffer. Purity of the plasmids was verified by absorbency at 260 and 280 nm and 1% agarose gel electrophoresis. The luciferase assay kit was from Promega (Madison, WI). The introducer and the 12 Fr sheath for image-guided catheter insertion were from COOK (Bloomington, IN) and the guide wire (ZIP wire) was from Boston Scientific (Natick, MA). Injection balloon catheters (10.5 Fr) were purchased from the Clinical Supply Co. (Kakamikahara, Gifu, Japan). The MIKRO TIP catheter transducer was from Millar (Houston, TX). Contrast medium (OXILAN) was from Guerbet (Bloomington, IN). WavelineVet Vital Signs Monitor for monitoring physiological parameters on animals was from DRE Veterinary (Louisville, KY). Pigs (female, 40–45 kg) were from Wally Whippo (Enon Valley, PA).

Animal catheterization. All animal experiments were conducted in full compliance with regulation of and approved by the Institutional Animal Care and Use Committee at the University of Pittsburgh, Pittsburgh, Pennsylvania. Under general anesthesia, animals were placed on the table of the fluoroscopy machine YSF-100 from Shimadzu Corp. (Nakagyo-ku, Kyoto, Japan). A 12 Fr short sheath was inserted in the jugular vein through a skin incision on the pigs. Following an insertion of the injection catheter, the balloon was inflated by injecting 1.5 ml of phase contrast medium. Obstruction of blood flow was verified by injecting a small volume of phase contrast medium into the vasculature through the catheter.

Hydrodynamic injection. Injections of saline containing either pCMV-Luc or pCAG-hAAT plasmid DNA (100 μg/ml), or phase contrast medium *via* the catheter were given to total of 42 pig livers by the *HydroJector* driven by the pressure provided by a gas (CO_2) cylinder with its pressure regulator set at 300 psi.[7,8] The venography was recorded using a VCR recorder connected to a fluoroscope. Intravascular pressure was transmitted to the computer using a MIKRO TIP catheter transducer inserted through the catheter to the hepatic veins. At the end of injection, the balloon remained inflated for 20 minutes and then slowly deflated. The sequential injection to multiple hepatic veins was performed with a 30 minutes interval in between. Animals received a postoperative analgesia with ketoprofen for 24 hours and an antibiotic with amoxicillin for 5 days.

Measurement of liver lobe volume. The RLL, RML, LML, and LLL in the pig liver was macroscopically identified and divided using deep interlobular and umbilical fissures according to segmental anatomy.[15,24] The CL was identified by the presence of the small fissure adjoining the RLL on the visceral surface according to previously reported method.[15] Three livers not injected with DNA were used to measure the volume of the liver lobes using water replacement method.[25] Average lobe volume of RLL, RML, and LLL were 0.54, 0.6, and 0.4% BW, respectively (liver density: ~1.00 kg/l).[26] The volume of each liver lobe for all animals used in the study was measured upon the euthanasia and the results coincided with predicted liver/body weight ratio.

Analysis of luciferase gene expression. Animals were euthanized and the liver was collected 24 hours after the hydrodynamic gene delivery of the pCMV-Luc plasmid. The luciferase and protein assays were performed according to the previously established procedure.[3] The level of reporter gene expression was obtained as the relative light units (RLU) converted to luciferase protein (ng) per mg of total proteins in tissue homogenate, using the equation derived from the standard curve in which luciferase protein (pg) = $7.98 \times 10^{-5} \times$ RLU + 0.093 ($R2$ = 0.9999).[3] A standard immunohistochemical staining was performed with a goat anti-luciferase polyclonal

antibody (G7451, 1:50 dilution; Promega, Madison, WI), Vecstatin Elite ABC Goat IgG Kit (PK–6105; Vector Laboratories, Burlingame, CA), and DAB chromogen tablet (Muto Pure Chemicals CO, Bunkyo-ku, Tokyo, Japan) for luciferase staining. Microscopic examination was performed and photo images were recorded using an imaging system (AxioImager A1, Carl Zeiss Microscopy GmbH, Jena, Germany).

Persistent transgene expression in hepatocytes. Pigs were euthanized on day 63 or 105 after the first hydrodynamic gene delivery of pCAG-hAAT, and liver samples were collected from various lobes for hAAT expression analysis. Ten liver tissue samples were collected from all lobes, and standard immunohistochemical staining was performed with a rabbit anti–hAAT antibody (ab9373, 1:20 dilution; Abcam, Cambridge, MA). Every three fields from each section were captured and a quantitative analysis of positively stained cells was performed using Image J software (version 1.6.0_20, National Institutes of Health) as previously reported.[16]

Genomic DNA isolation and PCR analysis. Sections of the livers, spleens, kidneys, brains, hearts, stomachs, colons, ovaries, lungs, muscles, and small intestines were collected and DNA was isolated using phenol–chloroform extraction. Multiplex PCR was carried out on the samples and as well as a vector DNA with Ampicillin resistance gene primers and glyceraldehyde 3-phosphate dehydrogenase (*Gapdh*) gene as a reference. 2 µl of sample were amplified in a 20 µl PCR reaction at the program for 10 minutes at 94 °C, and 35 cycles for 1 minute at 94 °C, 1 minute at 56 °C, 1 minute at 72 °C, followed by a 10-minute extension at 72 °C. The primers used in PCR analysis were: *Gapdh* (forward), AGGTCGGAGT GAACGGATTTG; *Gapdh* (reverse), TGTAGACCATGTAGTGG AGGTCA; *Amp* (forward), TACAGGCATCGTGGTGTCAC; and *Amp* (reverse), AAATGTGCGCGGAACCCCTA.

Assessment of tissue damage. Blood samples were collected from the ear or peripheral vein in the limb from pigs at appropriate time points. Automated concentration determination was performed by the Cleveland Office of Marshfield Labs. Hematoxylin & eosin staining was performed on the liver tissues in the pathology lab of the Department of Pathology, University of Pittsburgh.

Statistical analysis. The luciferase assays were statistically evaluated by the analysis of variance followed by Bonferronis multiple comparison test.

Supplementary material

Figure S1. Level of gene expression in left medial lobe.
Figure S2. Effect of repeat hydrodynamic injection on physiological parameters.

Acknowledgments. The authors would like to thank Michael Maranowski, Christopher Janssen and all staff members in the Division of Laboratory Animal Resources at the University of Pittsburgh for the excellent assistance in animal care. The authors would also like to thank Miss Ryan Fugett for the critical reading of the manuscript and English language review. The authors declare that they have no conflict of interest. The research in the authors' laboratory has been supported in part by grant support from the National Institute of Health (EB002946 and HL075542) to LD, and from the Japanese Society for the Promotion of Sciences (22890064 and 23790595), Takeda foundation, and Uehara Foundation to KK.

1. Kamimura, K and Liu, D (2008). Physical approaches for nucleic acid delivery to liver. *AAPS J* **10**: 589–595.
2. Kamimura, K, Suda, T, Zhang, G and Liu, D (2011). Advances in gene delivery systems. *Pharmaceut Med* **25**: 293–306.
3. Liu, F, Song, Y and Liu, D (1999). Hydrodynamics-based transfection in animals by systemic administration of plasmid DNA. *Gene Ther* **6**: 1258–1266.
4. Zhang, G, Budker, V and Wolff, JA (1999). High levels of foreign gene expression in hepatocytes after tail vein injections of naked plasmid DNA. *Hum Gene Ther* **10**: 1735–1737.
5. Suda, T and Liu, D (2007). Hydrodynamic gene delivery: its principles and applications. *Mol Ther* **15**: 2063–2069.
6. Herweijer, H and Wolff, JA (2007). Gene therapy progress and prospects: hydrodynamic gene delivery. *Gene Ther* **14**: 99–107.
7. Suda, T, Suda, K and Liu, D (2008). Computer-assisted hydrodynamic gene delivery. *Mol Ther* **16**: 1098–1104.
8. Kamimura, K, Suda, T, Xu, W, Zhang, G and Liu, D (2009). Image-guided, lobe-specific hydrodynamic gene delivery to swine liver. *Mol Ther* **17**: 491–499.
9. Yoshino, H, Hashizume, K and Kobayashi, E (2006). Naked plasmid DNA transfer to the porcine liver using rapid injection with large volume. *Gene Ther* **13**: 1696–1702.
10. Aliño, SF, Herrero, MJ, Noguera, I, Dasí, F and Sánchez, M (2007). Pig liver gene therapy by noninvasive interventionist catheterism. *Gene Ther* **14**: 334–343.
11. Eastman, SJ, Baskin, KM, Hodges, BL, Chu, Q, Gates, A, Dreusicke, R *et al.* (2002). Development of catheter-based procedures for transducing the isolated rabbit liver with plasmid DNA. *Hum Gene Ther* **13**: 2065–2077.
12. Fabre, JW, Grehan, A, Whitehorne, M, Sawyer, GJ, Dong, X, Salehi, S *et al.* (2008). Hydrodynamic gene delivery to the pig liver via an isolated segment of the inferior vena cava. *Gene Ther* **15**: 452–462.
13. Herrero, MJ, Sabater, L, Guenechea, G, Sendra, L, Montilla, AI, Abargues, R *et al.* (2012). DNA delivery to 'ex vivo' human liver segments. *Gene Ther* **19**: 504–512.
14. Khorsandi, SE, Bachellier, P, Weber, JC, Greget, M, Jaeck, D, Zacharoulis, D *et al.* (2008). Minimally invasive and selective hydrodynamic gene therapy of liver segments in the pig and human. *Cancer Gene Ther* **15**: 225–230.
15. Court, FG, Wemyss-Holden, SA, Morrison, CP, Teague, BD, Laws, PE, Kew, J *et al.* (2003). Segmental nature of the porcine liver and its potential as a model for experimental partial hepatectomy. *Br J Surg* **90**: 440–444.
16. Vrekoussis, T, Chaniotis, V, Navrozoglou, I, Dousias, V, Pavlakis, K, Stathopoulos, EN *et al.* (2009). Image analysis of breast cancer immunohistochemistry-stained sections using ImageJ: an RGB-based model. *Anticancer Res* **29**: 4995–4998.
17. The Journal of Gene Medicine. Gene therapy clinical trials worldwide. http://www.wiley.com/legacy/wileychi/genmed/clinical/ (Accessed on 27 February 2013).
18. Kamimura, K, Zhang, G and Liu, D (2010). Image-guided, intravascular hydrodynamic gene delivery to skeletal muscle in pigs. *Mol Ther* **18**: 93–100.
19. Brunetti-Pierri, N, Stapleton, GE, Palmer, DJ, Zuo, Y, Mane, VP, Finegold, MJ *et al.* (2007). Pseudo-hydrodynamic delivery of helper-dependent adenoviral vectors into non-human primates for liver-directed gene therapy. *Mol Ther* **15**: 732–740.
20. Aliño, SF, Crespo, A and Dasí, F (2003). Long-term therapeutic levels of human alpha-1 antitrypsin in plasma after hydrodynamic injection of nonviral DNA. *Gene Ther* **10**: 1672–1679.
21. Fairbanks, KD and Tavill, AS (2008). Liver disease in alpha 1-antitrypsin deficiency: a review. *Am J Gastroenterol* **103**: 2136–41; quiz 2142.
22. Zhang, G, Song, YK and Liu, D (2000). Long-term expression of human alpha1-antitrypsin gene in mouse liver achieved by intravenous administration of plasmid DNA using a hydrodynamics-based procedure. *Gene Ther* **7**: 1344–1349.
23. Flotte, TR and Mueller, C (2011). Gene therapy for alpha-1 antitrypsin deficiency. *Hum Mol Genet* **20**(R1): R87–R92.
24. Couinaud, C (1999). Liver anatomy: portal (and suprahepatic) or biliary segmentation. *Dig Surg* **16**: 459–467.
25. Heymsfield, SB, Fulenwider, T, Nordlinger, B, Barlow, R, Sones, P and Kutner, M (1979). Accurate measurement of liver, kidney, and spleen volume and mass by computerized axial tomography. *Ann Intern Med* **90**: 185–187.
26. Yuan, D, Lu, T, Wei, YG, Li, B, Yan, LN, Zeng, Y *et al.* (2008). Estimation of standard liver volume for liver transplantation in the Chinese population. *Transplant Proc* **40**: 3536–3540.

Supplementary Information accompanies this paper on the Molecular Therapy–Nucleic Acids website (http://www.nature.com/mtna)

Scandinavian Journal of Gastroenterology. 2013; Early Online, 1–7

informa
healthcare

ORIGINAL ARTICLE

Salvage endoscopic submucosal dissection in patients with local failure after chemoradiotherapy for esophageal squamous cell carcinoma

MANABU TAKEUCHI[1], MASAAKI KOBAYASHI[2], SATORU HASHIMOTO[2], KEN-ICHI MIZUNO[2], GEN KAWAGUCHI[3], RYUTA SASAMOTO[3], HIDEFUMI AOYAMA[3] & YUTAKA AOYAGI[1]

[1]*Departments of Gastroenterology, Niigata University Medical and Dental Hospital, Chuo-ku, Niigata, Japan,* [2]*Departments of Endoscopy, Niigata University Medical and Dental Hospital, Chuo-ku, Niigata, Japan, and* [3]*Departments of Radiology, Niigata University Medical and Dental Hospital, Chuo-ku, Niigata, Japan*

Abstract

Objective. For locoregional failure after chemoradiotherapy (CRT) in patients with esophageal squamous cell carcinoma (ESCC), salvage esophagectomy and endoscopic mucosal resection have disadvantages, such as a high morbidity rate and a high local recurrence rate, respectively. The aim of this study was to clarify the efficacy of salvage endoscopic submucosal dissection (ESD) for locoregional failure of CRT. ***Methods.*** A total of 19 lesions in 19 patients were treated with salvage ESD; 15 lesions were local recurrences at the primary site and 4 lesions were residual. All lesions were intramucosal or submucosal tumors without metastases. A case-control study was retrospectively evaluated to clarify whether the clinical outcomes of salvage ESD were equivalent to those of control primary ESD. ***Results.*** No significant differences were observed between salvage ESD and primary ESD in short-term outcomes, including procedure time. For salvage ESD, the complete *en bloc* resection rate was 94.7% (18 of 19), and no severe complications were observed. At a median follow up of 54.6 (range: 5–98) months after salvage ESD, the local recurrence rate was 0%. However, three patients (15.8%) died due to lymph node and distant metastases and six patients (31.5%) died from other diseases, including radiation pneumonitis, pyothorax or respiratory failure with no recurrence of ESCC. The 3-year overall survival rate for all 19 patients was 74%. ***Conclusions.*** ESD represents an acceptable treatment option for recurrent or residual ESCC because of its improvement in local control, when local failure after CRT is limited to the submucosal layer without metastases.

Key Words: *chemoradiotherapy, endoscopic submucosal dissection, esophageal squamous cell carcinoma, local failure, salvage therapy, survival rate*

Introduction

Chemoradiotherapy (CRT) is a curative standard treatment option for locally advanced esophageal squamous cell carcinoma (ESCC). It was reported that definitive CRT achieved 5-year survival rate of about 30% [1–3]. Locoregional recurrence or residual tumor occurs in >40% of patients who have undergone CRT [3–5]. Control in local failure without distant metastasis is a major factor for improving patient survival after CRT. Salvage esophagectomy has a curative potential for locoregional failure of CRT; however, it is associated with higher morbidity and mortality rates than primary esophagectomy [6–8]. Responses to second-line chemotherapy protocols are quite poor for such tumors.

It has been reported that salvage endoscopic mucosal resection (EMR) is one of the curative and minimally invasive treatments for recurrent or residual ESCC after CRT, when the locoregional tumor is superficial and local [9,10]. The 3- and 5-year survival rates for salvage EMR were 56% and 49%,

Correspondence: Manabu Takeuchi, MD, Department of Gastroenterology, Niigata University Medical and Dental Hospital, 1-754 Asahimachi-dori, Chuo-ku, Niigata 951-8520, Japan. Tel: +81 25 227 2207. Fax: +81 25 227 0776. E-mail: manabu@med.niigata-u.ac.jp

(Received 18 May 2013; revised 25 June 2013; accepted 27 June 2013)

ISSN 0036-5521 print/ISSN 1502-7708 online © 2013 Informa Healthcare
DOI: 10.3109/00365521.2013.822092

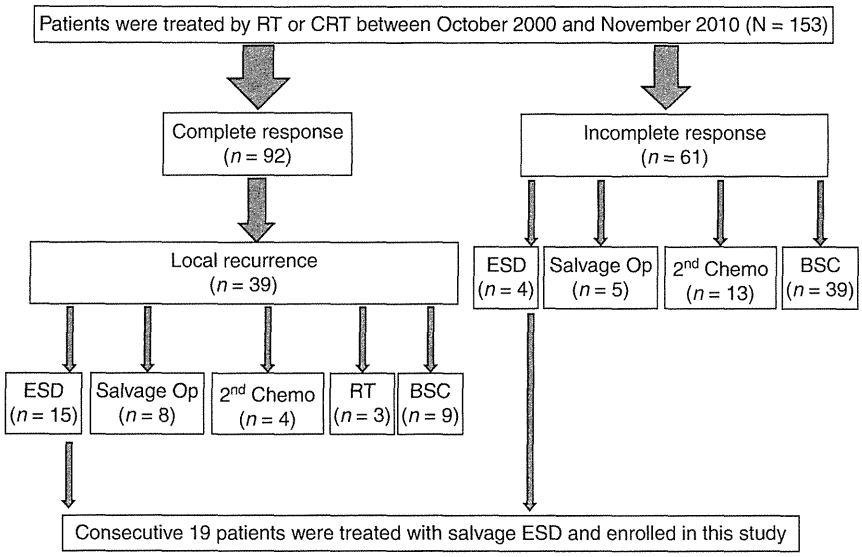

Figure 1. Flow diagram of 153 patients treated by initial CRT for esophageal cancer but affected with local failure as recurrent or residual. RT, radiotherapy; CRT, chemoradiotherapy; ESD, endoscopic submucosal dissection; Op, operation; 2nd Chemo, second-line chemotherapy; BSC, best supportive care.

respectively [10], which were similar to those for salvage esophagectomy. However, the limitations of salvage EMR include: (1) difficulty lifting due to CRT-induced submucosal fibrosis; (2) a low complete *en bloc* resection rate, even for small lesions; (3) positive vertical margins in submucosal invasive cancer; and (4) local recurrence after salvage EMR. Yano et al. evaluated the clinical outcome after salvage EMR for 21 patients with recurrent or residual tumors [10]. They reported that the *en bloc* resection rate for salvage EMR was 33%, the incomplete resection rate was 33%, and the local recurrence rate was 33%. Local recurrence requires further intervention after salvage EMR. Repeat endoscopic treatments may impose a burden on patients.

Endoscopic submucosal dissection (ESD) was developed as a new endoscopic treatment about 10 years ago. The major advantages of ESD include both an extremely high rate of *en bloc* resection and the possibility of resection for lesions with submucosal fibrosis [11,12]. However, little is known about whether salvage ESD has curative potential for recurrent or residual ESCC after CRT or whether it can be performed without complications. The efficacy of ESD as a salvage treatment for locoregional failures has been reviewed in a case series with limited numbers, and neither short- nor long-term survival data have been reported [13]. Therefore, the clinical outcomes, including the short- and long-term results of salvage ESD for recurrent or residual esophageal tumors after CRT, were retrospectively evaluated in our consecutive 19 case series.

Materials and methods

Patients

This study was initially composed of 153 patients diagnosed with ESCC between October 2000 and November 2010 at the Niigata University Medical and Dental Hospital, Niigata, Japan. Each patient was treated with radiotherapy, which primarily consisted of more than 50 Gy of irradiation with or without concurrent chemotherapy. Figure 1 shows the flow of patients with locoregional failure after CRT. Local recurrences developed at the primary site in 39 of 92 patients after a complete response to CRT, while 61 patients had residual lesions after an incomplete response to CRT. The definition of complete response at the primary site was determined as the complete disappearance of all measurable and assessable disease; incomplete partial response was defined as a reduction of measurable and assessable disease. Of the 100 patients, 15 patients with local recurrence at the primary site and 4 patients with residual lesions were selected for salvage ESD. The remaining patients were treated with either a salvage operation ($n = 13$), second-line chemotherapy ($n = 17$), second irradiation ($n = 3$), or best supportive care ($n = 48$), depending on the surgical resectability and the patient's general condition. All 19 patients selected for salvage ESD were treated between March 2005 and January 2013, and their clinical outcomes were retrospectively analyzed after ESD.

The baseline clinical characteristics of the 19 patients treated with salvage ESD are summarized

Table I. Baseline characteristics of primary esophageal cancer.

Tumor status before CRT	Recurrent (n = 15)	Residual (n = 4)
Sex (male/female)	14/1	4/0
Age, median years (range)	72 (52–91)	70 (61–76)
Location (U/M/L)	3/8/2004	0/3/1
Stage		
T1/T2/T3/T4	9/3/3/0	3/1/0/0
N0/N1	15/0	4/0
M0/M1	15/0	4/0
TNM (I/II/III/IV)	9/6/0/0	3/1/0/0
Time to CRT failure, median months (range)	11 (2–94)	Ð

Abbreviations: CRT = chemoradiotherapy; ESD = endoscopic submucosal dissection; U = upper; M = middle; L = lower.

in Table I. The baseline pre-CRT clinical stage of each patient was evaluated according to the criteria of TNM classification from the *International Union against Cancer Classification of Malignant Tumours* (7th edition) [14]. All locoregional tumors were diagnosed by endoscopic observation, including Lugol chromoendoscopy and magnified image-enhanced endoscopy, and histologically confirmed by the presence of cancer cells in biopsy specimens. To determine the depth of cancer invasion, endoscopic ultrasound using a 20 MHz ultrasound miniature-probe (UM-3R; Olympus Medical Systems, Tokyo, Japan) or magnifying endoscopy with narrow band imaging (H260Z; Olympus Medical Systems) was carried out. Computed tomography (CT) of the neck, chest, and abdomen was performed to evaluate lymph node or distant metastases. Lymph node metastasis was clinically defined in the current study as a lymph node >10 mm at its shortest dimension on CT.

Selection criteria for salvage ESD were: (1) depth of tumor limited to within the submucosal layer (clinical stage T1); (2) no evidence of lymph node or distant organ metastasis (clinical stage N0M0); (3) absence of other uncontrolled advanced cancers; and (4) written, informed consent obtained from the patient before study commencement.

This study was approved by the Hospital Clinical Ethics Committee. All information was collected from medical records or provided by the patients' physicians.

Salvage ESD procedure

Salvage ESD procedures were performed using a hook knife as the main device, as developed by Oyama et al. [11]. Glyceol® (Chugai Pharmaceutical Co., Tokyo, Japan) was used in each case as the submucosal injection solution to maintain proper submucosal elevation. ESD procedures were performed using video endoscopy (GIF-Q240, GIF-Q240Z, or GIF-Q260J; Olympus Medical Systems). A transparent disposable attachment (D-201-11804 or D-201-11304; Olympus Medical Systems) was fitted to the tip of the endoscope to retract the submucosal layer and facilitate dissection. Lesion margins were delineated before ESD using 0.6% iodine staining. After injection of a 10% glycerin solution that contained 0.005 mg/mL epinephrine into the submucosal layer, a mucosal incision at the distal side of the lesion was made using a hook knife. Before incising the mucosa of the entire lesion around the markings, one side of the lesion was longitudinally cut from proximal to distal. The submucosal layer beneath the area where the mucosal incision was made was then dissected. This procedure was repeated longitudinally from oral to anal, with the direction of the top of the hook knife controlled toward the mucosal incision site and kept parallel to the muscular layer, while slightly pushing the endoscope. The submucosal dissection of one side was continued until half or two-third of the lesion was completely dissected. Then, the mucosa of the other side of the lesion was incised, and the remaining submucosal layer was dissected as previously described [15]. To minimize the degree of variation in endoscopic practice, all resections were performed by two experienced senior endoscopists (M. T. and M. K.).

To clarify whether the short-term clinical outcomes of salvage ESD were equivalent to those of primary ESD, a case-control study was evaluated. The control group of 50 lesions treated with primary ESD was randomly selected during the same period in 50 patients. These lesions were matched in size and treatment year to the salvage ESD group. We evaluated ESD procedure time, histological findings, and complications as the short-term results.

Histological evaluation

Specimens taken at ESD were subsequently examined after being cut into slices 2 to 3 mm in width and microscopically assessed for histological type, depth of tumor invasion, vascular invasion, horizontal margin, and vertical margin. Complete resection was defined as *en bloc* resection free from both horizontal and vertical margins. Histopathological evaluations were performed according to Japanese classification of esophageal cancer [16].

Complications

The major complications typically associated with salvage ESD include major bleeding and perforation.

Table II. Clinical short-term outcomes of salvage ESD.

	Recurrent (n = 15)	Residual (n = 4)	Size-matched control (n = 50)
Procedure time, median min (range)	63 (36–128)	56 (32–120)	50 (28–111)
En-bloc resection	15 (100%)	4 (100%)	50 (100%)
Tumor-free margin			
Horizontal	15 (100%)	4 (100%)	50 (100%)
Vertical	14 (93%)	4 (100%)	50 (100%)
Tumor depth			
EP, LPM	8 (53%)	1 (25%)	31 (62%)
MM, SM1	3 (20%)	1 (25%)	12 (24%)
SM2	4 (27%)	2 (50%)	7 (14%)
Vascular invasion			
Venous	2 (13%)	1 (25%)	0 (0%)
Lymphatic	0	0	3 (6%)
Complication			
Perforation	0	0	0
Major bleeding	0	0	0

Abbreviations: EP = epithelium; LPM = lamina propria mucosae; MM = muscularis mucosae; SM1 = minimal submucosal layer; SM2 = massive submucosal layer.

In the present study, major bleeding was defined as bleeding that required blood transfusion or surgical intervention. Perforation was detected endoscopically or by the presence of subcutaneous emphysema on physical examination.

Follow-up examinations

Endoscopic follow-up examinations were carried out at 3, 6, and 12 months after salvage ESD, and every 6–12 months thereafter. CT follow up was also performed every 4–6 months after ESD. Local recurrence after salvage ESD was diagnosed when cancer cells were histologically proven in biopsy specimens obtained from the ESD scar. The recurrence of lymph node and/or distant metastases was determined on CT.

Statistics

Clinicopathological data of lesions were analyzed using a Mann–Whitney U test for numerical data and a $\chi 2$ test or Fisher's exact probability test for categorical data. Overall survival (OS) was measured from the date of initial salvage therapy to the date of death for any reason or the last follow-up visit. Survival time was evaluated by the Kaplan–Meier method. All statistical analyses were performed using IBM SPSS Statistics version 21 software (IBM Japan Inc., Tokyo, Japan).

Results

Clinical short-term outcomes of salvage ESD

The clinical results of salvage ESD according to tumor status after CRT are summarized in Table II. No significant differences were observed among the three groups (recurrent group, residual group, and size-matched control group). The median sizes of the removed specimens for the three groups were 15, 14, and 15 mm, respectively. In the 19 patients with local failure, overall median procedure time for salvage ESD was 62 (range, 32–128) min. *en bloc* resection was performed for all 19 lesions. Histopathological assessment of specimens taken at salvage ESD revealed that six lesions (31.6%) had massively invaded the submucosal layer and resected non-curatively due to positive vertical margin (n = 1) or positive venous invasion (n = 4). No immediate or delayed complications, including major bleeding or perforation, and no ESD-related deaths occurred in any patients. A representative case of a patient who underwent salvage ESD is shown in Figure 2.

The five patients with failure of salvage ESD due to positive vertical margin or positive venous invasion might have been eligible for salvage surgery. However, these patients did not undergo any further treatment because of their general condition or refusal, except for one patient who was treated with additional chemotherapy.

Clinical course after salvage ESD

At a median follow-up time of 54.6 (range: 5–98) months, no local recurrence had developed at the treatment site in any patient. Overall, 10 of 19 patients (52.6 %) were still alive and disease-free after salvage ESD, but three patients with massive submucosal invasion had died from lymph node and distant metastases. In two of the three patients, histological examination showed venous invasion and infiltrative growth patterns. The remaining six patients had died

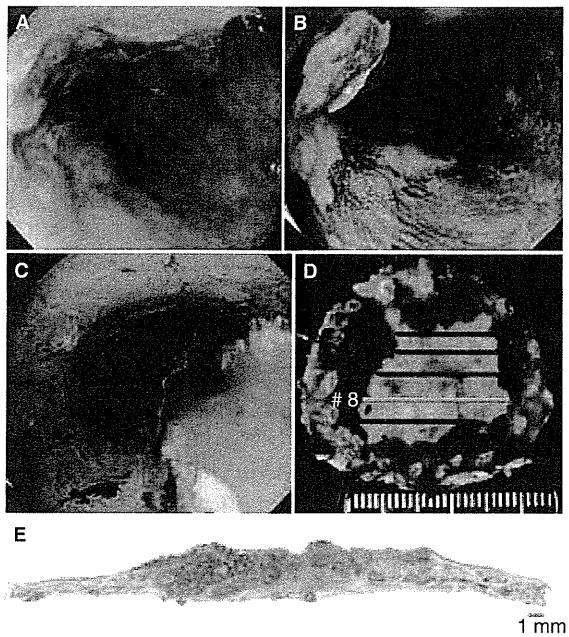

Figure 2. Representative case of a patient who achieved salvage ESD. (A) Esophagoscopy before CRT showed ulcerative and localized type squamous cell carcinoma at the middle-third esophagus. (B) Endoscopic examination with iodine staining 3 months after CRT showed an elevated residual lesion, where the depth was suspected to be at the submucosal layer. (C) Salvage ESD using a hook knife was performed with *en bloc* resection. There was neither bleeding nor perforation. (D) The fixed resected specimen after iodine staining. (E) Histopathological examination showed that both lateral and vertical margins were negative and there was massive depth invasion in the submucosal layer.

from other diseases, including radiation pneumonitis, pyothorax, or respiratory failure with no recurrence of ESCC. The 3-year OS rates after salvage ESD were 74% (Figure 3).

Discussion

Salvage ESD for recurrent or residual superficial esophageal carcinoma after CRT achieved a high rate of complete resection. No complications, such as perforation or major bleeding, were observed. Accurate histopathological evaluation of the resected specimen was crucial to determine a surveillance strategy. These benefits emphasized the advantage of ESD compared with salvage chemotherapy, radiotherapy, and conventional EMR. The short- and long-term results from salvage ESD were within acceptable limits. Therefore, when locoregional failure is limited to the submucosal layer with no metastases, salvage ESD represents an acceptable treatment option that provides efficacy, safety, and curability, requiring a certain level of ESD expertise.

The most important advantage of the ESD technique, compared with conventional EMR, is that neoplasms with submucosal fibrosis, such as ulcerative non-lifting neoplasms and recurrent neoplasms, are resectable. Although EMR for lesions with submucosal fibrosis is difficult due to poor submucosal lifting, with sufficient injection, the ESD procedure permits dissection of the fibrous connective tissue of the submucosa beneath the lesion under direct visualization. Moreover, ESD also enables us to achieve a negative vertical margin in 86% (six of seven) lesions with massive submucosal invasion. In the present study, all locoregional lesions had submucosal fibrosis, including submucosal invasion, but no local recurrence was performed at a median follow up of 55 months. Some endoscopists and oncologists may believe that salvage ESD is a more time-consuming and invasive procedure. However, in the present study, no significant differences were observed

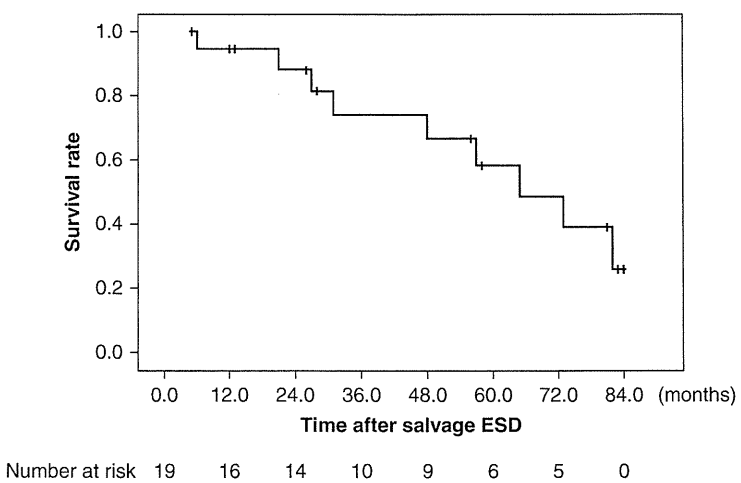

Figure 3. OS of 19 patients from salvage ESD.

between salvage ESD and primary ESD procedure time, and *en bloc* resection rate and the incidence of margin involvement resulted in a high curability rate. These results suggest that salvage ESD is more feasible than salvage EMR in terms of curative potential.

The complications following ESD include major bleeding and perforation. In the present study, no cases of severe bleeding requiring blood transfusion or perforation were seen after salvage ESD. In previous studies, the rate of esophageal perforation with ESD was between 0% and 6.9% [11,12,17]. It is technically more difficult to perform salvage ESD than initial ESD, because severe fibrosis forms beneath the mucosal layer after CRT. Therefore, salvage ESD should be performed carefully to avoid incomplete resection or perforation.

Several studies have reported results of salvage photodynamic therapy (PDT) for persistent or recurrent local disease in esophageal cancer after CRT [18]. Complete response rates ranged between 20% and 100%, with local recurrence seen in 12–28% of patients. Significant complications were seen in some studies, including death, mediastinitis, perforation, tracheoesophageal fistula, and stenosis requiring dilation. Salvage PDT requires significant endoscopic expertise and access is limited to specialized tertiary care centers.

The 5-year survival rate of patients after salvage esophagectomy has been reported to be over 50% when the locoregional disease is pathologically proven to be T1 or T2 without lymph node or distant metastasis [5]. The present study resulted in a 3-year survival rate after salvage ESD of 74%. This result suggests that salvage ESD has a curative potential for early stage local failure after CRT. However, a disease-free state was not achieved in three patients with lymph node and distant metastases, even after complete resection by salvage ESD. These three patients had massive submucosal invasion of residual ($n = 2$) or recurrent ($n = 1$) cancers and were positive for venous invasion ($n = 2$). Therefore, if high-risk factors can be identified from the ESD specimen of patients of a well-general condition, additional chemotherapy immediately after ESD may be beneficial. It is important to recognize that baseline ESCC showed less advanced stages in patients with salvage ESD. Therefore, we cannot conclude from this study that ESD had a better survival rate than other treatments. The main factor for the good result of this study may be the selection criteria for salvage ESD. We treated only 19 of 100 patients with recurrent or residual esophageal cancers, who were strictly suitable as having clinical stage T1N0M0 after CRT.

This retrospective study did have some limitations. The number of patients that required salvage ESD was small, since many patients with locoregional failure after CRT also had distant or lymph node metastases and/or deeper invasion that could not be removed by ESD. While the patient series was not large, the outcome data may be meaningful, especially as many patients with recurrent and residual ESCC are poor surgical candidates due to advanced age and/or comorbidities. A further limitation of our study is that all resections were performed by two experienced senior endoscopists. Further long-term follow-up studies will be required to define the population of patients who are most likely to benefit from this treatment.

In conclusion, salvage ESD in a tertiary care center demonstrated acceptable short-term safety and worthwhile curative properties when used in treating local failures after CRT. Therefore, due to its therapeutic improvement in local control, salvage ESD represents a promising treatment option for residual or recurrent carcinoma.

Declaration of interest: All authors declare no financial relationships or conflicts of interest.

References

[1] Chan A, Wong A. Is combined chemotherapy and radiation therapy equally effective as surgical resection in localized esophageal carcinoma? Int J Radiat Oncol Biol Phys 1999; 45:265–70.

[2] Cooper JS, Guo MD, Herskovic A, Macdonald JS, Martenson JA, Al-Sarraf M, et al. Chemoradiotherapy of locally advanced esophageal cancer: long-term follow-up of a prospective randomized trial (RTOG 85-01). Radiation Therapy Oncology Group. JAMA 1999;281:1623–7.

[3] Herskovic A, Martz K, Al-Sarraf M, Leichman L, Brindle J, Vaitkevicius V, et al. Combined chemotherapy and radiotherapy compared with radiotherapy alone in patients with cancer of the esophagus. N Engl J Med 1992;326:1593–8.

[4] Bedenne L, Michel P, Bouche O, Milan C, Mariette C, Conroy T, et al. Chemoradiation followed by surgery compared with chemoradiation alone in squamous cancer of the esophagus: FFCD 9102. J Clin Oncol 2007;25:1160–8.

[5] Stahl M, Stuschke M, Lehmann N, Meyer HJ, Walz MK, Seeber S, et al. Chemoradiation with and without surgery in patients with locally advanced squamous cell carcinoma of the esophagus. J Clin Oncol 2005;23:2310–17.

[6] Swisher SG, Wynn P, Putnam JB, Mosheim MB, Correa AM, Komaki RR, et al. Salvage esophagectomy for recurrent tumors after definitive chemotherapy and radiotherapy. J Thorac Cardiovasc Surg 2002;123:175–83.

[7] Miyata H, Yamasaki M, Takiguchi S, Nakajima K, Fujiwara Y, Nishida T, et al. Salvage esophagectomy after definitive chemoradiotherapy for thoracic esophageal carcinoma. J Surg Oncol 2009;100:442–6.

[8] Tachimori Y, Kanamori N, Uemura N, Hokamura N, Igaki H, Kato H. Salvage esophagectomy after high-dose

chemoradiotherapy for esophageal squamous cell carcinoma. J Thorac Cardiovasc Surg 2009;137:49–54.

[9] Hattori S, Muto M, Ohtsu A, Boku N, Manabe T, Doi T, et al. EMR as salvage treatment for patients with locoregional failure of definitive chemoradiotherapy for esophageal cancer. Gastrointest Endosc 2003;58:65–70.

[10] Yano T, Muto M, Hattori S, Minashi K, Onozawa M, Nihei K, et al. Long-term results of salvage endoscopic mucosal resection in patients with local failure after definitive chemoradiotherapy for esophageal squamous cell carcinoma. Endoscopy 2008;40:717–21.

[11] Oyama T, Tomori A, Hotta K, Morita S, Kominato K, Tanaka M, et al. Endoscopic submucosal dissection of early esophageal cancer. Clin Gastroenterol Hepatol 2005;3:67–70.

[12] Fujishiro M, Yahagi N, Kakushima N, Kodashima S, Muraki Y, Ono S, et al. Endoscopic submucosal dissection of esophageal squamous cell neoplasms. Clin Gastroenterol Hepatol 2006;4:688–94.

[13] Saito Y, Takisawa H, Suzuki H, Takizawa K, Yokoi C, Nonaka S, et al. Endoscopic submucosal dissection of recurrent or residual superficial esophageal cancer after chemoradiotherapy. Gastrointest Endosc 2008;67:355–9.

[14] Sobin LH, Gospodarowicz MK, Wittekind C. editors. TNM classification of malignant tumours. 7th edition. Oxford: Wiley-Blackwell; 2009. pp. 66–72.

[15] Takeuchi M, Kobayashi M, Hashimoto S, Sato Y, Narisawa R, Aoyagi Y. The strategy of endoscopic submucosal dissection for the esophageal carcinoma on abdominal esophagus. Esophagus 2010;7:173–6.

[16] Japan Esophageal Society. Japanese classification of esophageal cancer, 10th edition: part I. Esophagus 2009; 6:1–25.

[17] Ishihara R, Iishi H, Uedo N, Takeuchi Y, Yamamoto S, Yamada T, et al. Comparison of EMR and endoscopic submucosal dissection for en bloc resection of early esophageal cancers in Japan. Gastrointest Endosc 2008;68: 1066–72.

[18] Khangura SK, Greenwald BD. Endoscopic management of esophageal cancer after definitive chemoradiotherapy. Dig Dis Sci 2013;58:1477–85.

Hindawi Publishing Corporation
Case Reports in Medicine
Volume 2013, Article ID 298143, 7 pages
http://dx.doi.org/10.1155/2013/298143

Hindawi

Case Report

Immunohistochemical Character of Hepatic Angiomyolipoma: For Its Management

Yuka Kobayashi,[1] Kenya Kamimura,[2] Minoru Nomoto,[2] Soichi Sugitani,[1] and Yutaka Aoyagi[2]

[1] *Division of Gastroenterology, Tachikawa General Hospital, Kandamachi 3-2-11, Nagaoka, Niigata 940-8621, Japan*
[2] *Division of Gastroenterology and Hepatology, Graduate School of Medical and Dental Sciences, Niigata University, Asahimachi 1-757, Chuo-ku, Niigata, Niigata 951-8122, Japan*

Correspondence should be addressed to Yuka Kobayashi; ykoba-gi@umin.ac.jp

Received 9 April 2013; Revised 9 May 2013; Accepted 28 May 2013

Academic Editor: Sarkis Meterissian

Hepatic angiomyolipoma (AML) is notoriously difficult to diagnose without an invasive surgery even with the recent development of the various imaging modalities. Additionally, recent reports showed its malignant behavior after the surgery; it is important to diagnose the character of each tumor including the possible malignant potential and determine the postoperative management for each case. For this purpose, we have reviewed reports and focused on the immunohistochemical staining with p53 and ki67 of the tumors showing the representative case of 60-year-old female. The imaging study of her tumor showed the character similar to the hepatocellular carcinoma, and she underwent the hepatectomy. The resected tumor stained positive for HMB-45 that is a marker of the AML, and 30–50% of the tumor cells were positively stained with Ki67 that is a mitotic marker. Also, the atypical epithelioid cells displayed p53 immunoreactivity. These results suggest the malignant potential of our tumor based on the previous reports; therefore the careful followup for this case is necessary for a long period whether it shows metastasis, sizing up, and so forth.

1. Introduction

Angiomyolipoma of the liver is rare and has been considered a benign tumor since Ishak [1] first described the condition in 1976. The tumor has three cellular components: fat cells, smooth muscle cells, and blood vessels. However, the proportion of these three components varies considerably from case to case and from area to area within the same tumor. The classification of malignant liver tumors is often very difficult due to the phenotypic variability of the fatty portion [2–4]. In histological preparations, the smooth muscle cell element of the tumor exhibits variable morphological features with occasional atypical cells. These tumors are frequently misdiagnosed as malignant neoplasms. It is well known that an invasive growth pattern is one of the most important histological features differentiating malignant from benign tumors. Although the majority of hepatic AML are clinically benign, invasive growth features are frequently found in hepatic AML [5]. However, malignant hepatic AML is extremely rare; distant metastasis and tumor recurrence are rarely reported. Dalle et al. reported a 70-year-old patient with hepatic AML that showed prominent vascular invasion histologically, and the patient died of recurrent disease with multiple liver and peritoneal metastases [6]. Certain hepatic AML characteristics may be associated with malignant potential. These include tumor size, portal vein thrombus, marked cell proliferation, and p53 immunoreactivity, p53 mutations [7, 8]. Based on these facts, although the imaging studies have been developed with the new modalities, the histological diagnosis and the surgical treatment still play a key role to determine the management strategy for each case. Therefore, in this paper, showing the representative case, we reviewed the literature and discussed the importance of the immunohistochemical staining with p53 and ki67 for the management of this tumor.

2. Diagnosis of Hepatic AML

Among the various benign tumors, angiomyolipoma (AML) is a well-known renal tumor associated with the tuberous

sclerosis complex. However, such tumors have been reported to occur in various extrarenal sites, including the liver, uterus, and retroperitoneum. Hepatic AML is a rare benign tumor of mixed mesenchymal origin, which Ishak [1] firstly described in 1976. The disease is asymptomatic in 60% of patients; abdominal pain is the most common symptom [9, 10]. Due to the variable amount of adipose tissue in each tumor, it is sometimes difficult to distinguish between benign and malignant tumors by imaging studies. Without the information provided by a surgical examination, it is possible to misdiagnose hepatic AML as a lipoma, hepatocellular carcinoma, sarcoma, or metastasis [11, 12]. While reviewing these reports, we have summarized the typical imaging findings for hepatic AML as follows: (1) ultrasonography (US) evidence of a heterogeneously hyperechoic mass, (2) plain computed tomography (CT) sign of a heterogeneously area of low density, and (3) magnetic resonance imaging (MRI) showing various images depending on the component of tumor tissue. High intensity on the T2-weighted image and high or low intensity on the T1-weighted image are observed based on the amount of adipose tissue contained. The adipose tissue is determined by the low-intensity area revealed in the out-of-phase and fat suppression images [13–16], (4) tumor staining and hypervascularity as revealed by angiography [13, 14]. Although a combination of US, abdominal CT, MRI, and angiography increases diagnostic accuracy, only 25%–52% of preoperative diagnoses are correct [15, 16]. Therefore, the definitive diagnosis is only possible postoperatively due to the need for histological verification. Even then, hepatic AML is often mistaken as hepatocellular carcinoma since it is rare. Identification of smooth muscle cells, blood vessels, and adipose tissue with a positive immunohistochemical reaction for HMB-45 is the final evidence for an angiomyolipoma [17–19]. The majority of hepatic AMLs invade the surrounding tissue. In this case, the intraoperative view revealed invasive growth, with hepatic cord hepatocyte replacement and extension into the portal area and/or around hepatic veins [5].

The biological behavior of hepatic AML requires further investigation. Because hepatic AML has been considered as benign tumor, most clinicians advocated conservative treatment. In 2000, Dalle et al. reported the first case of malignant hepatic AML [6], in a 70-year-old patient with hepatic AML that showed prominent vascular invasion upon histological examination. The patient died of recurrent disease with multiple liver and peritoneal metastases 7 months after the surgery. Since then, several authors have reported that hepatic AML is likely to metastasize, enlarge, and recur. Therefore, it is not prudent to treat hepatic AML as a simple benign tumor. At the very least, the physicians must be aware of the potential for malignant transformation.

We reviewed the literature [20, 21] and here summarized the similarities and differences between classic and malignant hepatic AML (Table 1). Both classic and malignant hepatic AML possess three basic components that can be visualized through histological investigation: blood vessels, fat cells, and epithelioid-spindle cells. Both types of hepatic AML express smooth muscle and melanocytic markers, such as α-SMA and HMB-45. In the nine cases that have been published, all of which clearly involved metastasis and/or recurrence, the malignant hepatic AML was >8 cm in diameter. Some cases involved portal vein thrombus and necrosis. A recent study by Maklouf et al. showed that CD117 staining was positive in all cases of benign renal and hepatic AML [22]. Nguyen et al. reported a loss of CD117 expression as a sign of hepatic AML malignancy [20]. Deng et al. reported that the central hepatic AML lesion could be identified as atypical epithelioid components with pleomorphic and frequent mitotic figures, p53 immunoreactivity, and p53 mutations at exon 7. High levels of p53 expression are often associated with malignancy, which means that positive p53 staining may signal impending metastasis [21]. Mizuguchi et al. stain for HMB-45 and Ki67, a mitotic marker, to identify hepatic AML malignancy [23]. Although all these findings support the existence of malignant hepatic AML, the reports leave many questions unanswered. Therefore, we are focusing on the immunohistochemical character of hepatic AML to predict its malignant potential for the decision of the management of the tumor.

3. Representative Case

Our representative case was a 60-year-old woman. She had no history of malignant disease, and the blood exams were negative for tumor markers and viral markers.

3.1. Imaging Studies. The abdominal plain CT revealed a low-density area (Figure 1(a)) in segment 6 of the liver, and a dynamic study revealed a remarkably hypervascular tumor, which stained in the early phase (Figure 1(b)) and showed a vaguely defective area with minimal high-density staining in the late phase (Figures 1(c) and 1(d)). Abdominal ultrasonography was not performed. T1-weighted magnetic resonance imaging (MRI) depicted the tumor as an area of low signal intensity on in-phase (Figure 2(a)) and as a low-intensity lesion on out-of-phase (Figure 2(b)). Interestingly, the relative signal loss in out-of-phase is detected compared to the in-phase, probably due to the presence of the adipose tissue in the tumor. In diffusion-weighted images, the tumor was identified as an area of high signal intensity (Figures 2(c) and 2(d)). Dynamic contrast enhancement MRI with a hepatocyte-specific contrast agent (gadolinium-ethoxybenzyl-diethylenetriamine pentaacetic acid) revealed hypervascularity and early enhancement of the tumor. Hepatic cell phase images revealed defective areas within the tumor (Figures 3(a)–3(d)). On the basis of these imaging studies and the tumor location, we suspected malignancy associated with a hepatocellular carcinoma; therefore, she underwent the partial hepatectomy.

3.2. Pathology. A partial hepatectomy of segment 6 was performed. Upon macroscopic examination, the surgical specimen appeared as a solid whitish mass consisting of a single nodule free of necrosis. There were no signs of chronic inflammation or fibrosis in the surrounding liver tissue. The three defining characteristics of AML were identified, including mature fat, blood vessels, and epithelioid-spindle cells (Figures 4(a)–4(c)). The round or polygonal tumor cells

Table 1: Characteristics for malignant AML.

	Classic AML components	Atypical AML components
Tumor size [7]		>5 cm
Pathological		
Cell atypical	−	+
Invasion in hepatic parenchyma	±	+
Portal venous tumor thrombus [7]	−	+
Necrosis [20]	−	+
Immunohistochemical		
HMB-45	+	+
α-SMA	+	+
Ki67 [23]	<5%	>30%
p53 [21]	−	>10%
CD117 [20]	+	−

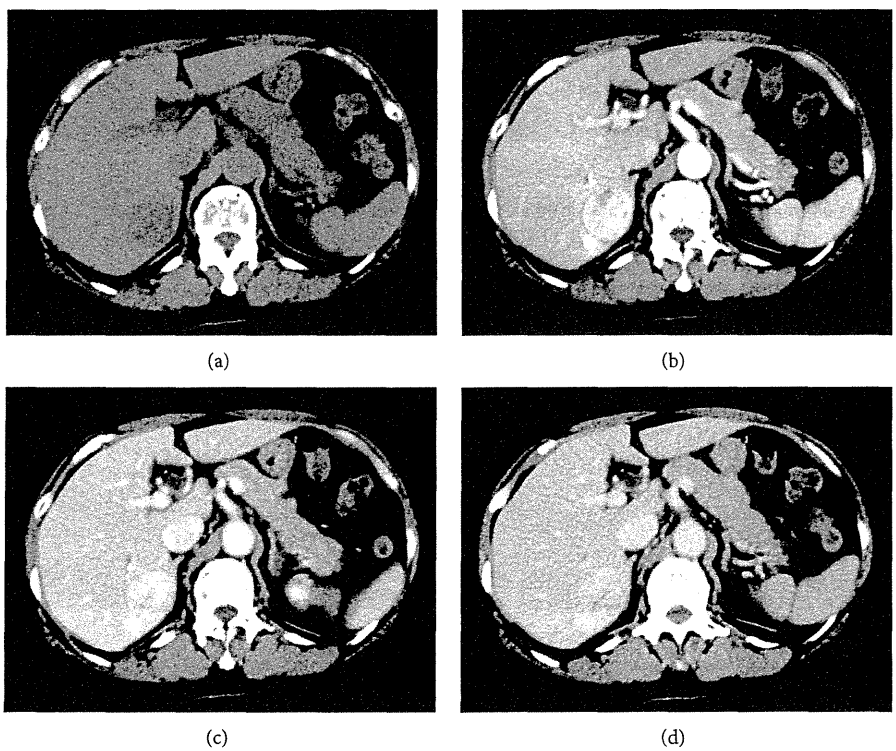

Figure 1: Dynamic contrast enhancement computed tomography (CT). Plain CT revealed a low-density tumor in segment 6 (a). Tumor hypervascularity in the arterial phase (b). Hypervascular lesions remained in the portal phase (c) and late phase (d).

were arranged in a sheet, with sign of tumor invasion at the tumor-nontumor interface (Figure 4(d)). Tumor cells had replaced hepatocytes within the liver cell cords along the hepatic sinusoids. In addition, small isolated clusters of tumor cells were occasionally found proximal to the main tumor mass, suggesting tumor sprouting. The tumor was positive for HMB-45 (Figures 5(a) and 5(b)), a marker of AML, vimentin, and α-SMA (Figures 5(c) and 5(d)). Fat cells and blood vessels were observed as well, and interestingly p53-positive cells were scattered diffusely throughout the tumor (Figure 6(a)), and 30%–50% of cells in the solid region of the tumor were positive for Ki67 (Figure 6(b)). Based on the literature review described above, we diagnosed that this hepatic AML might have a malignant potential, therefore, this patient is being

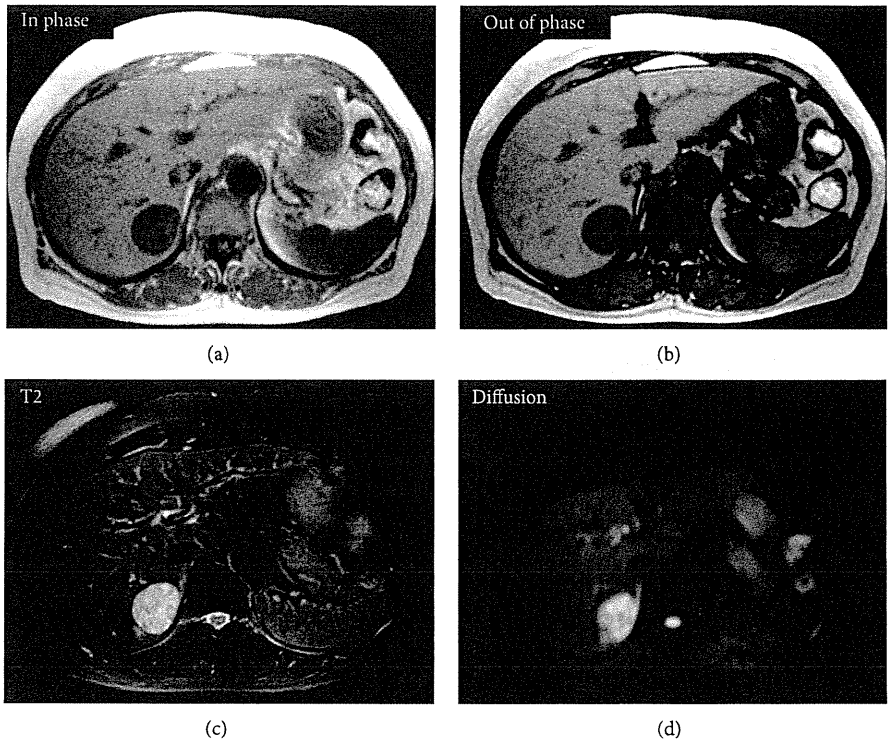

FIGURE 2: Magnetic resonance imaging. The tumor appeared as a low-intensity area on T1-weighted in-phase (a) and out-of-phase images (b). On T2-weighted with fat saturation and diffusion-weighted images, the tumor appeared as an area of high intensity ((c), (d)).

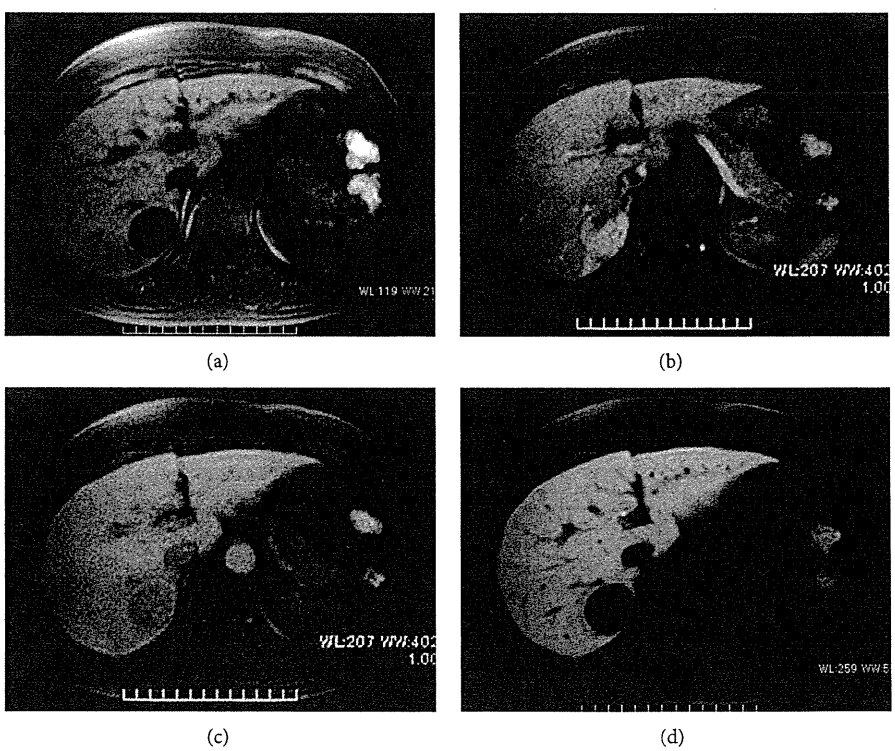

FIGURE 3: Dynamic contrast enhancement MRI with a hepatocyte-specific contrast agent (gadolinium-ethoxybenzyl-diethylenetriamine pentaacetic acid). Plain T1-weighted MRI revealed a low-intensity tumor (a), arterial phase hypervascularity (b), and a defective area visible in the late phase (c) and in the hepatic cellular phase (d).

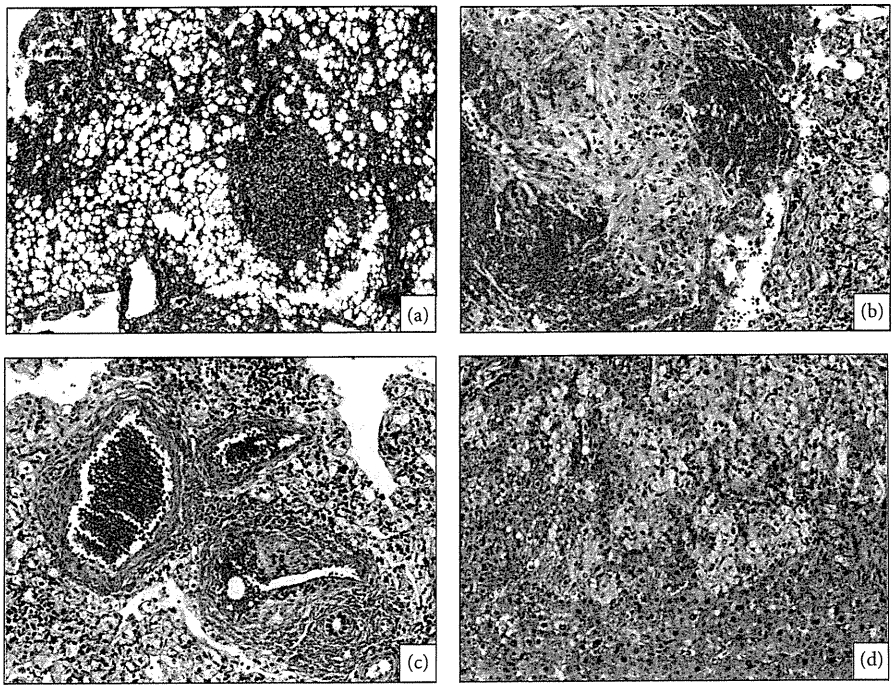

FIGURE 4: Histological findings (HE staining): the tumor included mature fat, blood vessels, and epithelioid-spindle cells (×120) (a). A part of the tumor showed predominance of spindle cells and blood vessel (×120) (b) (×300) (c). The tumor showed invasive growth pattern (×300) (d).

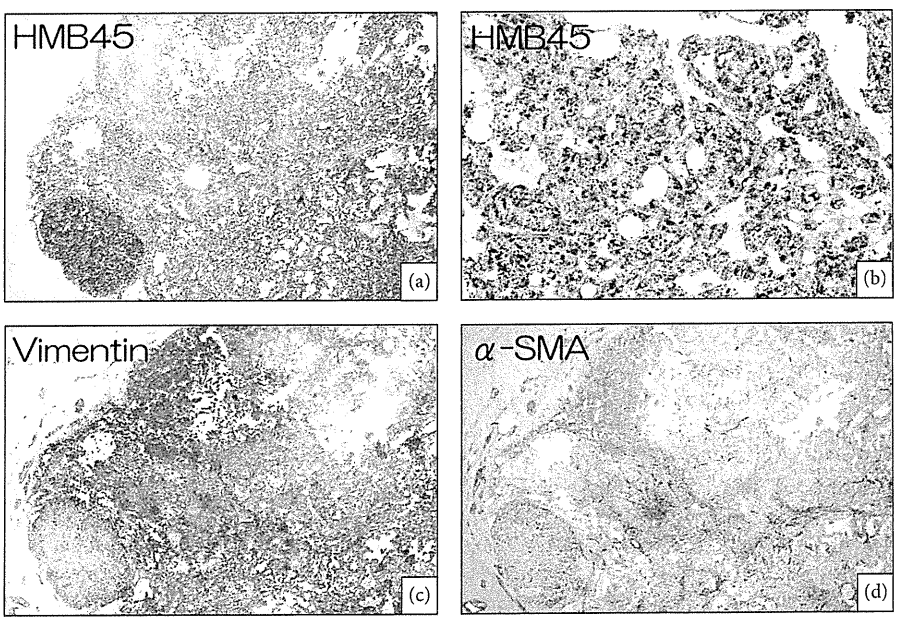

FIGURE 5: Immunopathological characteristics: tumor cells were positive for HMB-45 staining (×120) (a), (×1200) (b), for vimentin staining (×120) (c), and for α-SMA staining (×120) (d).

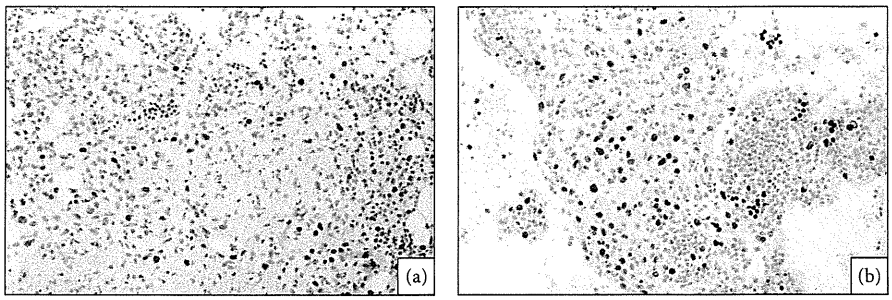

FIGURE 6: Immunopathological characteristics: approximately 5% of atypical epithelioid cells were positive for p53 (×1200) (a), and more than 30% of epithelioid cells were immunoreactive for Ki67 (×1200) (b).

followed carefully at our hospital, and, to date, there has been no evidence of postoperative recurrence or metastasis.

4. Conclusion

Hepatic AML usually follows a benign clinical course. However, the tumor malignancy cannot be ignored. Therefore, we recommend that excision or fine-needle biopsy be accompanied by subsequent histological staining for markers such as Ki67 and p53. This information will be helpful for the management of the tumor.

Conflict of Interests

The authors declare that they have no current financial arrangement or affiliation with any organization that may have a direct influence on their work.

References

[1] K. G. Ishak, "Mesenchymal tumors of the liver," in *Hepatocellular Carcinoma*, pp. 247–307, John Wiley & Sons, New York, NY, USA, 1976.

[2] A. Nonomura, Y. Mizukami, and M. Kadoya, "Angiomyolipoma of the liver: a collective review," *Journal of Gastroenterology*, vol. 29, no. 1, pp. 95–105, 1994.

[3] Z. D. Goodman and K. G. Ishak, "Angiomyolipomas of the liver," *American Journal of Surgical Pathology*, vol. 8, no. 10, pp. 745–750, 1984.

[4] A. Nonomura, Y. Mizukami, K. Muraoka, M. Yajima, and K. Oda, "Angiomyolipoma of the liver with pleomorphic histological features," *Histopathology*, vol. 24, no. 3, pp. 279–281, 1994.

[5] A. Nonomura, Y. Enomoto, M. Takeda et al., "Invasive growth of hepatic angiomyolipoma; a hitherto unreported ominous histological feature," *Histopathology*, vol. 48, no. 7, pp. 831–835, 2006.

[6] I. Dalle, R. Sciot, R. De Vos et al., "Malignant angiomyolipoma of the liver: a hitherto unreported variant," *Histopathology*, vol. 36, no. 5, pp. 443–450, 2000.

[7] K. Kamimura, A. Oosaki, S. Sugahara et al., "Malignant potential of hepatic angiomyolipoma: case report and literature review," *Clinical Journal of Gastroenterology*, vol. 3, no. 2, pp. 104–110, 2010.

[8] K. Kamimura, M. Nomot, and Y. Aoyagi, "Hepatic angiomyolipoma: diagnostic findings and management," *International Journal of Hepatology, Article*, vol. 2012, Article ID 410781, 6 pages, 2012.

[9] G.-H. Ding, Y. Liu, M.-C. Wu, G.-S. Yang, J.-M. Yang, and W.-M. Cong, "Diagnosis and treatment of hepatic angiomyolipoma," *Journal of Surgical Oncology*, vol. 103, no. 8, pp. 807–812, 2011.

[10] Y.-M. Zhou, B. Li, F. Xu et al., "Clinical features of hepatic angiomyolipoma," *Hepatobiliary and Pancreatic Diseases International*, vol. 7, no. 3, pp. 284–287, 2008.

[11] T. Messiaen, C. Lefebvre, B. Van Beers, C. Sempoux, J. P. Cosyns, and A. Geubel, "Hepatic angiomyo(myelo)lipoma: difficulties in radiological diagnosis and interest of fine needle aspiration biopsy," *Liver*, vol. 16, no. 5, pp. 338–341, 1996.

[12] L. Xie, J. Jessurun, J. C. Manivel, and S. E. Pambuccian, "Hepatic epithelioid angiomyolipoma with trabecular growth pattern: a mimic of hepatocellular carcinoma on fine needle aspiration cytology," *Diagnostic Cytopathology*, vol. 40, no. 7, pp. 639–650, 2012.

[13] S. Sajima, H. Kinoshita, K. Okuda et al., "Angiomyolipoma of the liver—a case report and review of 48 cases reported in Japan," *Kurume Medical Journal*, vol. 46, no. 2, pp. 127–131, 1999.

[14] S. Krebs, I. Esposito, C. Lersch, J. Gaa, R. M. Schmid, and O. Ebert, "Preoperative radiological characterization of hepatic angiomyolipoma using magnetic resonance imaging and contrast-enhanced ultrasonography: a case report," *Journal of Medical Case Reports*, vol. 26, no. 5, article 481, 2011.

[15] Z.-G. Chang, J.-M. Zhang, J.-Q. Ying, and Y.-P. Ge, "Characteristics and treatment strategy of hepatic angiomyolipoma: a series of 94 patients collected from four institutions," *Journal of Gastrointestinal and Liver Diseases*, vol. 20, no. 1, pp. 65–69, 2011.

[16] G.-H. Ding, Y. Liu, M.-C. Wu, G.-S. Yang, J.-M. Yang, and W.-M. Cong, "Diagnosis and treatment of hepatic angiomyolipoma," *Journal of Surgical Oncology*, vol. 103, no. 8, pp. 807–812, 2011.

[17] B. Terris, J.-F. Fléjou, R. Picot, J. Belghiti, and D. Hénin, "Hepatic angiomyolipoma: a report of four cases with immunohistochemical and DNA-flow cytometric studies," *Archives of Pathology and Laboratory Medicine*, vol. 120, no. 1, pp. 68–70, 1996.

[18] W. M. S. Tsui, A. K. T. Yuen, K. F. Ma, and C. C. H. Tse, "Hepatic angiomyolipomas with a deceptive trabecular pattern and HMB-45 reactivity," *Histopathology*, vol. 21, no. 6, pp. 569–573, 1992.

[19] P. Flemming, U. Lehmann, T. Becker, J. Klempnauer, and H. Kreipe, "Common and epithelioid variants of hepatic

angiomyolipoma exhibit clonal growth and share a distinctive immunophenotype," *Hepatology*, vol. 32, no. 2, pp. 213–217, 2000.

[20] T. T. Nguyen, B. Gorman, D. Shields, and Z. Goodman, "Malignant hepatic angiomyolipoma: report of a case and review of literature," *American Journal of Surgical Pathology*, vol. 32, no. 5, pp. 793–798, 2008.

[21] Y.-F. Deng, Q. Lin, S.-H. Zhang, Y.-M. Ling, J.-K. He, and X.-F. Chen, "Malignant angiomyolipoma in the liver: a case report with pathological and molecular analysis," *Pathology Research and Practice*, vol. 204, no. 12, pp. 911–918, 2008.

[22] H. R. Makhlouf, H. E. Remotti, and K. G. Ishak, "Expression of KIT (CD117) in angiomyolipoma," *American Journal of Surgical Pathology*, vol. 26, no. 4, pp. 493–497, 2002.

[23] T. Mizuguchi, T. Katsuramaki, T. Nobuoka et al., "Growth of hepatic angiomyolipoma indicating malignant potential," *Journal of Gastroenterology and Hepatology*, vol. 19, no. 11, pp. 1328–1330, 2004.

World Journal of Gastroenterology

Online Submissions: http://www.wjgnet.com/esps/
wjg@wjgnet.com
doi:10.3748/wjg.v19.i24.3831

World J Gastroenterol 2013 June 28; 19(24): 3831-3840
ISSN 1007-9327 (print) ISSN 2219-2840 (online)

BRIEF ARTICLE

Active treatments are a rational approach for hepatocellular carcinoma in elderly patients

Takeshi Suda, Aiko Nagashima, Shyunsaku Takahashi, Tsutomu Kanefuji, Kenya Kamimura, Yasushi Tamura, Masaaki Takamura, Masato Igarashi, Hirokazu Kawai, Satoshi Yamagiwa, Minoru Nomoto, Yutaka Aoyagi

Takeshi Suda, Aiko Nagashima, Shyunsaku Takahashi, Tsutomu Kanefuji, Kenya Kamimura, Yasushi Tamura, Masaaki Takamura, Masato Igarashi, Hirokazu Kawai, Satoshi Yamagiwa, Minoru Nomoto, Yutaka Aoyagi, Division of Gastroenterology and Hepatology, Graduate School of Medical and Dental Sciences, Niigata University, Chuo-ku, Niigata, Niigata 951-8122, Japan

Author contributions: Suda T designed the research, analyzed the data and wrote the paper; Nagashima A, Takahashi S, Kanefuji T, Kamimura K, Tamura Y, Takamura M, Igarashi M, Kawai H and Yamagiwa S collected the data; Nomoto M and Aoyagi Y critically discussed the paper based on their expertise.

Correspondence to: Dr. Takeshi Suda, Division of Gastroenterology and Hepatology, Graduate School of Medical and Dental Sciences, Niigata University, 1-757 Asahimachi-dori, Chuo-ku, Niigata, Niigata 951-8122, Japan. suda@med.niigata-u.ac.jp
Telephone: +81-25-2272207 Fax: +81-25-2270776
Received: January 4, 2013 Revised: February 10, 2013
Accepted: April 28, 2013
Published online: June 28, 2013

Abstract

AIM: To determine whether an active intervention is beneficial for the survival of elderly patients with hepatocellular carcinoma (HCC).

METHODS: The survival of 740 patients who received various treatments for HCC between 1983 and 2011 was compared among different age groups using Cox regression analysis. Therapeutic options were principally selected according to the clinical practice guidelines for HCC from the Japanese Society of Hepatology. The treatment most likely to achieve regional control capability was chosen, as far as possible, in the following order: resection, radiofrequency ablation, percutaneous ethanol injection, transcatheter arterial chemoembolization, transarterial oily chemoembolization, hepatic arterial infusion chemotherapy, systemic chemotherapy including molecular targeting, or best supportive care. Each treatment was used alone, or in combination, with a clinical goal of striking the best balance between functional hepatic reserve and the volume of the targeted area, irrespective of their age. The percent survival to life expectancy was calculated based on a Japanese national population survey.

RESULTS: The median ages of the subjects during each 5-year period from 1986 were 61, 64, 67, 68 and 71 years and increased significantly with time ($P < 0.0001$). The Child-Pugh score was comparable among younger (59 years of age or younger), middle-aged (60-79 years of age), and older (80 years of age or older) groups ($P = 0.34$), whereas the tumor-node-metastasis stage tended to be more advanced in the younger group ($P = 0.060$). Advanced disease was significantly more frequent in the younger group compared with the middle-aged group ($P = 0.010$), whereas there was no difference between the middle-aged and elderly groups ($P = 0.75$). The median survival times were 2593, 2011, 1643, 1278 and 1195 d for 49 years of age or younger, 50-59 years of age, 60-69 years of age, 70-79 years of age, or 80 years of age or older age groups, respectively, whereas the median percent survival to life expectancy were 13.9%, 21.9%, 24.7%, 25.7% and 37.6% for each group, respectively. The impact of age on actual survival time was significant ($P = 0.020$) with a hazard ratio of 1.021, suggesting that a 10-year-older patient has a 1.23-fold higher risk for death, and the overall survival was the worst in the oldest group. On the other hand, when the survival benefit was evaluated on the basis of percent survival to life expectancy, age was again found to be a significant explanatory factor ($P = 0.022$); however, the oldest group showed the best survival among the five different age groups. The youngest group revealed the worst outcomes in this analysis, and the hazard ratio of the oldest against the youngest was 0.35 for death. The survival trends did not differ substantially between the survival time and percent survival to

life expectancy, when survival was compared overall or among various therapeutic interventions.

CONCLUSION: These results suggest that a therapeutic approach for HCC should not be restricted due to patient age.

Key words: Hepatocellular carcinoma; Population aging; Survival; Life expectancy; Active intervention

Core tip: Progressive population aging worldwide demands consensus development for decision making to treat elderly patients. A simple comparison of survival days is confounded by aging; therefore, age compensation is mandatory to evaluate survival benefits among different age groups. In this study, age difference was compensated by life expectancy in a hepatocellular carcinoma cohort. The authors suggested that age itself might not be a critical determinant for the selection of a therapeutic option. This study emphasizes the importance of clarifying risk determinants specific for elderly patients with respect to individual aspects and medical economy.

Suda T, Nagashima A, Takahashi S, Kanefuji T, Kamimura K, Tamura Y, Takamura M, Igarashi M, Kawai H, Yamagiwa S, Nomoto M, Aoyagi Y. Active treatments are a rational approach for hepatocellular carcinoma in elderly patients. *World J Gastroenterol* 2013; 19(24): 3831-3840 Available from: URL: http://www.wjgnet.com/1007-9327/full/v19/i24/3831.htm DOI: http://dx.doi.org/10.3748/wjg.v19.i24.3831

INTRODUCTION

The Japanese population is aging more rapidly than that of any other nation in the world. In 1990, approximately one in eight people in Japan were aged 65 years or older[1]. This level was already the highest in Asia, although somewhat lower than in most developed European countries. Since then, the population of Japan has aged because of an increasing life expectancy and a falling birth rate[2]. As a result, as many as one in four of the Japanese population will be at least 65 years old by the year 2025[3], which is a much higher ratio than that predicted for any other country.

There is much controversy concerning medical interventions for elderly patients. Zhang *et al*[4] reported that an interventional scheme should not be changed on the basis of the age of patients facing the treatment of myocardial infarction, whereas Teo *et al*[5] reported that the addition of percutaneous coronary intervention to optimal medical therapy did not improve the clinical outcomes in patients 65 years of age or older. An active treatment is recommended for elderly patients suffering from subarachnoid hemorrhage[6,7]. However, a conservative treatment was reported to be superior for elderly patients in the management of traumatic dental axis fracture[8]. Although some benefit of active treatment for hepatocellular carcinoma (HCC) in elderly patients has been suggested, the debate still continues as to how fast patients suffering from HCC are actually getting older and whether the survival benefit offered by active interventions is comparable between the young and the elderly.

In this report, aging trends among patients actively treated for HCC were evaluated over 25 years from 1986 to 2011 at a single institution in Japan. To compare the survival benefits between the relatively young and the elderly, survival was compared after adjusting the absolute survival time or life expectancy. Finally, a case presentation of an elderly patient who was successfully managed is used to illustrate the risks and benefits of active interventions for HCC in elderly patients.

MATERIALS AND METHODS

Patients

Clinicopathological data were retrospectively analyzed for 918 patients who were admitted between 1983 and 2011 for the first time for management of HCC in our hospital. The subjects' basic characteristics are shown in Table 1. To compare the ages of patients during each 5-year interval of the overall study period, 840 patients were selected who were admitted between 1986 and 2010. Only 740 patients who had already died or who had been followed for longer than a year in our hospital were included in survival analyses using actual survival time. Among these 740 cases, 504 could be allocated a life expectancy because these data are available for each age and gender since 1996 in Japan. To compare survival among different age groups, patients were classified into five groups according to their ages; 49 years of age or younger (-49), 50-59 years of age (50s), 60-69 years of age (60s), 70-79 years of age (70 s) and 80 years of age or older (80+).

Hepatic nodules were radiographically diagnosed as HCC when they fulfilled at least one of the following criteria based on dynamic computed tomography (CT)/magnetic resonance imaging and/or CT during hepatic arteriography/CT during arterial portography: (1) the typical hemodynamics of classical HCC, with a substantial arterial phase enhancement followed by a washout with a corona-like peripheral enhancement in an equilibrium phase; or (2) with similar characteristics as coexisting nodules that had already been diagnosed as HCC. Otherwise, a histological diagnosis was made.

Therapeutic options were principally selected according to the clinical practice guidelines for HCC from the Japanese Society of Hepatology, 2009[9]. The treatment most likely to achieve regional control capability was chosen, as far as possible, in the following order: resection, radiofrequency ablation (RFA), microwave coagulation (MWC), percutaneous ethanol injection (PEI), transcatheter arterial chemoembolization (TACE), transarterial oily chemoembolization (TOCE), hepatic arterial infusion chemotherapy (HAIC), systemic chemotherapy including molecular targeting or best supportive care. Each treatment was used alone or in combination, such as RFA af-